Journal of Organometallic Chemistry 880 (2019) 116–123

Contents lists available at ScienceDirect

Journal of Organometallic Chemistry

journal homepage: www.elsevier.com/locate/jorganchem

Photoluminescence of platinum(II) diethynylphenanthroline organometallic complexes with bis-arylethynyl derivatives in solution and solid state

Michito Shiotsuka*, Rikuo Ono, Yoshihiro Kurono, Taiki Asano, Yusuke Sakae

Graduate School of Engineering, Nagoya Institute of Technology, Gokiso, Showa, Nagoya, Aichi, 466-8555, Japan

ARTICLE INFO

Article history:
Received 14 September 2018
Received in revised form
24 October 2018
Accepted 31 October 2018
Available online 2 November 2018

Keywords:
Platinum
Luminescence
Organometallic complex
Aggregation-induced emission

ABSTRACT

Platinum(II) phenanthroline organometallics, Pt(3,8-Phen≡H)(≡Ph-R)$_2$ (**1H**–**11H**), of 11 respective arylethynyl ligands with different substituents: R = H (**1H**), 4-F (**2H**), 3-F (**3H**), 2-F (**4H**), 4-Me (**5H**), 4-CF_3 (**6H**), NO_2 (**7H**), 4-COOMe (**8H**), 4-*t*-Bu (**9H**), 3,5-di-CF_3 (**10H**), and 3,5-di-*t*-Bu (**11H**) were prepared from our reported complexes, Pt(3,8-Phen≡TMS)(≡Ph-R)$_2$, by a deprotection reaction of a trimethylsilyl group. The luminescence and the DFT calculations of the 11 present organometallics clearly supported the assignment of phosphorescence from the mixed transition of ^{3}MLCT/^{3}LLCT (LLCT = ligand-to-ligand charge transfer) in solution state. In solid state, the emission maximum peak values in the spectra of many complexes in 22 platinum organometallics occurred in the long wavelength area over 700 nm, and their emissions were assigned the phosphorescence from the transition of a metal-metal-to-ligand charge transfer, the so-called ^{3}MMLCT. This is related to the diversity of intermolecular interactions as Pt-Pt and π-π interactions in solid state. On the other hand, the emission peak values in the spectra of some complexes occurred in the short-wavelength area less than 600 nm. The complex Pt(3,8-Phen≡TMS)(≡Ph-3,5-di-CF_3)$_2$ showed a particularly strong and vibronic emission, and this phenomenon is presumed to be attributable to the aggregation-induced emission.

1. Introduction

Research into phosphorescent metal complexes continues to inspire highly efficient phosphorescence suitable for potential applications in a lot of sensing applications for environmental and biological technologies as well as the field of organic light-emitting diodes [1–5]. Phosphorescent studies of square-planar platinum(II) complexes have been reported by many groups because of the high emission quantum yield and long emission lifetime of platinum(II) complexes in solution and solid states [1–3,5–9]. In particular, platinum(II) organometallic complexes with bipyridine derivatives and various arylethynyl ligands, Pt(L)(≡-aryl)$_2$ (L = bipyridine derivatives), have recently received attention for their unique emissive properties such as aggregation-induced emission (AIE), vapochromism, and mechanochromism in solid state [10–14]. Photophysical studies of these platinum(II) organometallic complexes indicated that the emission of these complexes in solution was attributable to the mixed transition of ^{3}MLCT and ^{3}LLCT (LLCT = ligand-to-ligand charge transfer) from the photo-excited state [15]. On the other hand, some kinds of platinum(II) complexes Pt(L)(≡-aryl)$_2$ in solid state have shown phosphorescence from the transition of a metal-metal-to-ligand charge transfer (so-called ^{3}MMLCT) caused by the Pt-Pt interaction and, furthermore, unique luminescent properties such as vapochromism and mechanochromism [10–15]. As a part of this research trend, we recently reported the photophysics of platinum(II) organometallic complexes with phenanthroline derivatives and 11 respective arylethynyl ligands with a different substituent, Pt(3,8-Phen≡TMS)(≡Ph-R)$_2$ (3,8-Phen≡TMS = 3,8-bis-(trimethylsilyl)ethynyl-1,10-phenanthroline) (**1TMS** – **11TMS**), as shown in Scheme 1, and a good linear correlation has been revealed between the observed emission energy values of phosphorescence and the calculation values by DFT or TD-DFT in solution state [16]. Then, the emission spectra for some complexes of **1TMS** – **11TMS** in solid state showed phosphorescence from ^{3}MMLCT, and the phosphorescence was influenced by using various arylethynyl ligands with different substituents because the bulkiness of their substituents on respective arylethynyl

* Corresponding author.
E-mail address: michito@nitech.ac.jp (M. Shiotsuka).

https://doi.org/10.1016/j.jorganchem.2018.10.032
0022-328X/

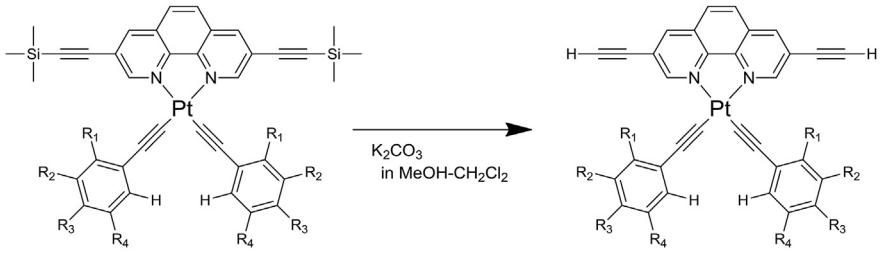

n = 1: R_1, R_2, R_3, R_4 = H
2: R_3 = F; R_1, R_2, R_4 = H
3: R_2 = F; R_1, R_3, R_4 = H
4: R_1 = F; R_2, R_3, R_4 = H
5: R_3 = CH_3; R_1, R_2, R_4 = H
6: R_3 = CF_3; R_1, R_2, R_4 = H
7: R_3 = NO_2; R_1, R_2, R_4 = H
8: R_3 = COOMe; R_1, R_2, R_4 = H
9: R_3 = $C(CH_3)_3$; R_1, R_2, R_4 = H
10: R_2, R_4 = CF_3 ; R_1, R_3 = H
11: R_2, R_4 = $C(CH_3)_3$, R_1, R_3 = H

Scheme 1. Synthetic route of platinum complexes **1H**–**11H** from precursor complexes **1TMS** – **11TMS**.

ligands affected the strength of the Pt-Pt interaction in the solid state of these compounds. Furthermore, Ni and coworkers recently reported the reversible vapochromism based on the similar platinum complex Pt(3,8-Phen≡TMS)(≡Ph-4-Cl)$_2$ [17]. We therefore became interested in the phosphorescence of platinum(II) organometallic complexes with phenanthroline and arylethynyl ligands having different degrees of bulkiness.

We report herein the synthesis and photophysical characterization of novel platinum(II) organometallic complexes with phenanthroline derivatives and 11 respective arylethynyl ligands with different substituents (Pt(3,8-Phen≡H)(≡Ph-R)$_2$ (3,8-Phen≡H = 3,8-diethynyl-1,10-phenanthroline): R = H (**1H**), 4-F (**2H**), 3-F (**3H**), 2-F (**4H**), 4-Me (**5H**), 4-CF_3 (**6H**), 4-NO_2 (**7H**), 4-COOMe (**8H**), 4-*t*-Bu (**9H**), 3,5-di-CF_3 (**10H**), 3,5-di-*t*-Bu (**11H**)), as shown in Scheme 1. The ligand 3,8-Phen≡H is flat and not bulkier than 3,8-Phen≡TMS; therefore, strong Pt-Pt interaction in solid state could be expected. The 11 present substituents of arylethynyl ligands were included from the bulky group as tertiary butyl substituents to the smallest substituent of hydrogen for the evaluation of the steric hindrance effect in solid state. Furthermore, the colors under white light and emissions under UV light of the 22 platinum complexes in solid state revealed the intermolecular Pt-Pt interactions and AIE in solid state. We measured the solid-state luminescent spectra of the 22 complexes and discussed the phosphorescence from ^{3}MMLCT caused by the Pt-Pt interaction and/or the mixed transition of ^{3}MLCT/^{3}LLCT. We also show a good linear correlation between phosphorescent energy measured by luminescence spectroscopy in solution state and the T_1-S_0 energy separation obtained by DFT or TD-DFT calculation of the present complexes Pt(3,8-Phen≡H)(≡Ph-R)$_2$.

2. Experimental section

2.1. Material and measurements

All chemicals used for syntheses were purchased from Aldrich or TCI and used without further purification. All reactions were carried out under an argon atmosphere. Solvents for the reaction were freshly distilled according to standard procedures. The syntheses of precursor complexes (Pt(3,8-Phen≡TMS)(≡Ph-R)$_2$: R = H (**1TMS**), 4-F (**2TMS**), 3-F (**3TMS**), 2-F (**4TMS**), 4-Me (**5TMS**), 4-CF_3 (**6TMS**), 4-NO_2 (**7TMS**), 4-COOMe (**8TMS**), 4-*t*-Bu (**9TMS**), 3,5-di-CF_3 (**10TMS**), 3,5-di-*t*-Bu (**11TMS**)) have been reported by our previous paper [16]. The characterization of the novel platinum complexes has been done by IR, ^{1}H NMR, UV–Vis spectroscopy, and elemental analyses. Elemental analyses for platinum complexes were performed for C, H, and N elements on a Elementar vario EL cube. IR spectra were obtained on a JASCO FT/IR 460 spectrometer using the KBr-pellet method. The ^{1}H NMR spectra were recorded with a Bruker AVANCE and Ascend™ NMR spectrometer (400 MHz) at room temperature and the chemical shifts were referenced to CD_2Cl_2 (5.320 ppm). UV–Vis spectra were recorded on a SHIMADZU UV-1800 spectrophotometer in CH_2Cl_2 (emission spectroscopic grade) at room temperature.

The corrected emission spectra in solution were measured with a HAMAMATSU C7473 photonic multi-channel analyzer and excitation spectra were recorded on a HITACHI F-2500 fluorescence spectrophotometer. Emission spectra for quantum yield measurement at room temperature were measured in a degassed CH_2Cl_2 (Emission spectral grade) by argon bubbling (over 15 min) upon excitation at 425 nm. Luminescence life times of present complexes at room temperature in a degassed CH_2Cl_2 were measured upon excitation at 355 nm YAG laser by UNISOKUTSP-2000. Emission spectra at 77 K were measured using a liquid nitrogen in a quarts Dewar vessel upon excitation at 425 nm and sample solutions (distilled 2-methyl-THF) in a 5 mm quarts sealed tube were deaerated by freeze-pump-thaw (over 3 times). The emission spectra in solid state were measured with HAMAMATSU Quantaurus-QY C11347-02. All solid samples were performed by the reprecipitation from CH_2Cl_2 solution and dried at 60 °C under vacuum for 4 h. TG-DTA measurement was performed all complexes until 300 °C by RIGAKU TG-DTA TG8120.

DFT and TD-DFT calculations were carried out using the program package *Gaussian 09 Revision C01* [18] at the B3LYP level with PCM method in CH_2Cl_2 solution and the calculation methods were performed with same condition of our previous paper [16]. The energy separation, E(T_1-S_0)$_{DFT}$, between the triplet (T_1) state and the singlet ground (S_0) state was obtained from the energy difference between the highest SOMO under T_1 state and HOMO under S_0 state for comparing phosphorescent energy from the emission spectral data of these complexes. TD-DFT calculation was also performed with restricted B3LYP in CH_2Cl_2 for the comparison between the calculated lowest triplet transition energy, E(T_1-S_0)$_{TD\text{-}DFT}$, and emission spectral data. The 6-31G(d) basis set was used for C, N, O, F, and H atoms, while the effective core potential and the associated valence basis set was employed with a LanL2DZ basis set for the Pt atom. The spatial plots of MOs were obtained with the program *GaussView 09* [18].

2.2. Preparations of platinum organometallics 1H–11H

2.2.1. Preparation of Pt(3,8-Phen≡H)(≡Ph)$_2$ (**1H**)

The **1TMS** (161 mg, 0.20 mmol) was dissolved in CH_2Cl_2 (20 mL) and added MeOH solution (40 mL) containing K_2CO_3 (30–39 mg,

0.22–0.28 mmol). After the mixture was stirred at r.t. for 3 h, the precipitate was filtered through filter paper and washed with water and diethyl ether. The yellow powder was obtained and dried at 60 °C under vacuum for 4 h. Yield: 122 mg (98%).

: Anal. Calcd for $C_{32}H_{18}N_2Pt$ 3/4CH_2Cl_2: C, 57.07; H, 2.85; N, 4.06. Found: C, 56.67; H, 2.78; N, 3.97%. FT-IR (KBr, cm^{-1}) ν(C≡C): 2117, ν(≡C-H): 3291. UV/VIS (CH_2Cl_2): λ_{abs} nm ($\varepsilon \times 10^{-5}$) 257 (0.66), 283 (0.71), 314 (0.40), 459 (0.07). ^{1}H NMR (CD_2Cl_2, 400 MHz, ppm): δ = 10.08 (d, 2H, J = 1.6 Hz, Phen-H2 and H9), 8.75 (d, J = 1.6 Hz, 2H, Phen-H4 and H7), 8.02 (s, 2H, Phen-H5 and H6), 7.55 (d, J = 8.0 Hz, 4H, Ph-H2 and H6), 7.32 (m, 4H, Ph-H3 and H5), 7.22 (d, J = 8.0 Hz, 2H, Ph-H4), 3.64 (s, 2H, Phen≡H).

*2.2.2. Preparation of Pt(3,8-Phen≡H)(≡Ph-4-F)$_2$ (**2H**)*

The Pt(3,8-Phen≡H)(≡Ph-4-F)$_2$ was synthesized by the same procedure to that for **1H** except for the use of **2TMS** (161 mg, 0.20 mmol). The orange brown powder is obtained. Yield: 126 mg (95%).

: Anal. Calcd for $C_{32}H_{16}N_2F_2Pt$ 1/2CH_2Cl_2: C, 55.45; H, 2.43; N, 3.98. Found: C, 55.31; H, 2.08; N, 3.71%. FT-IR (KBr, cm^{-1}) ν(C≡C): 2117, ν(≡C-H): 3299. UV/VIS (CH_2Cl_2): λ_{abs} nm ($\varepsilon \times 10^{-5}$) 255 (0.57), 282 (0.56), 313 (0.32), 459 (0.06). ^{1}H NMR (CD_2Cl_2, 400 MHz, ppm): δ = 10.03 (d, J = 1.6 Hz, 2H, Phen-H2 and H9), 8.75 (d, J = 1.6 Hz, 2H, Phen-H4 and H7), 8.02 (s, 2H, Phen-H5 and H6), 7.52 (dd, J = 5.5, 9.0 Hz, 4H, Ph-H2 and H6), 7.03 (t, J = 9.0 Hz, 4H, Ph-H3 and H5), 3.64 (s, 2H, Phen≡H).

*2.2.3. Preparation of Pt(3,8-Phen≡H)(≡Ph-3-F)$_2$ (**3H**)*

The Pt(3,8-Phen≡H)(≡Ph-3-F)$_2$ was synthesized with half scale by the same procedure to that for **1H** except for the use of **3TMS** (81 mg, 0.10 mmol). The orange powder was obtained. Yield: 64 mg (97%).

: Anal. Calcd for $C_{32}H_{16}N_2F_2Pt$ 1/4CH_2Cl_2: C, 56.73; H, 2.44; N, 4.10. Found: C, 56.80; H, 2.03; N, 3.98%. FT-IR (KBr, cm^{-1}) ν(C≡C): 2116, ν(≡C-H): 3297. UV/VIS (CH_2Cl_2): λ_{abs} nm ($\varepsilon \times 10^{-5}$) 261 (0.53), 284 (0.56), 310 (0.36), 454 (0.06). ^{1}H NMR (CD_2Cl_2, 400 MHz, ppm): δ = 9.83 (d, J = 1.6 Hz, 2H, Phen-H2 and H9), 8.67 (d, J = 1.6 Hz, 2H, Phen-H4 and H7), 7.98 (s, 2H, Phen-H5 and H6), 7.30 (m, 2H, Ph-H5), 7.29 (m, 2H, Ph-H6), 7.20 (m, 2H, Ph-H2), 6.95 (m, 2H, Ph-H4), 3.64 (s, 2H, Phen≡H).

*2.2.4. Preparation of Pt(3,8-Phen≡H)(≡Ph-2-F)$_2$ (**4H**)*

The Pt(3,8-Phen≡H)(≡Ph-2-F)$_2$ was synthesized with half scale by the same procedure to that for **1H** except for the use of **4TMS** (81 mg, 0.10 mmol). The yellow orange powder was obtained. Yield: 64 mg (97%).

: Anal. Calcd for $C_{32}H_{16}N_2F_2Pt$ 1/4CH_2Cl_2: C, 56.73; H, 2.44; N, 4.10. Found: C, 56.63; H, 2.05; N, 3.77%. FT-IR (KBr, cm^{-1}) ν(C≡C): 2123, ν(≡C-H): 3294. UV/VIS (CH_2Cl_2): λ_{abs} nm ($\varepsilon \times 10^{-5}$) 255 (0.50), 284 (0.52), 310 (0.36), 453 (0.06). ^{1}H NMR (CD_2Cl_2, 400 MHz, ppm): δ = 10.12 (d, J = 1.6 Hz, 2H, Phen-H2 and H9), 8.71 (d, J = 1.6 Hz, 2H, Phen-H4 and H7), 8.00 (s, 2H, Phen-H5 and H6), 7.56 (ddd, J = 1.6 and 8.0 Hz, 2H, Ph-H3), 7.18 (m, 2H, Ph-H5), 7.13 (d, J = 8.0 Hz, 2H, Ph-H6), 7.11 (tdd, J = 1.6, 3.2, 8.0 Hz, 2H, Ph-H4), 3.64 (s, 2H, Phen≡H).

*2.2.5. Preparation of Pt(3,8-Phen≡H)(≡Ph-4-Me)$_2$ (**5H**)*

The Pt(3,8-Phen≡H)(≡Ph-4-Me)$_2$ was synthesized with half scale by the same procedure to that for **1H** except for the use of **5TMS** (80 mg, 0.10 mmol). The red powder was obtained. Yield: 64 mg (98%).

: Anal. Calcd for $C_{34}H_{22}N_2Pt$ 1/4CH_2Cl_2: C, 60.96; H, 3.36; N, 4.15. Found: C, 60.93; H, 3.56; N, 3.84%. FT-IR (KBr, cm^{-1}) ν(C≡C): 2115, ν(-CH_3): 2862, 2918, ν(≡C-H): 3292. UV/VIS (CH_2Cl_2): λ_{abs} nm ($\varepsilon \times 10^{-5}$) 258 (0.68), 284 (0.72), 318 (0.41), 469 (0.07). ^{1}H NMR (CD_2Cl_2, 400 MHz, ppm): δ = 9.92 (d, 2H, J = 1.7 Hz, Phen-H2 and H9), 8.68 (d, J = 1.7 Hz, 2H, Phen-H4 and H7), 7.98 (s, 2H, Phen-H5 and H6), 7.42 (d, J = 8.0 Hz, 4H, Ph-H2 and H6), 7.15 (d, J = 8.0 Hz, 4H, Ph-H3 and H5), 3.62 (s, 2H, Phen≡H), 2.38 (s, 6H, Ph-CH_3).

*2.2.6. Preparation of Pt(3,8-Phen≡H)(≡Ph-4-CF_3)$_2$ (**6H**)*

The **6TMS** (80 mg, 0.06 mmol) was dissolved in CH_2Cl_2 (10 mL) and added MeOH solution (20 mL) containing K_2CO_3 (9.1–11.6 mg, 0.07–0.08 mmol). After the mixture solution was stirred at r.t. for 3 h, the solution was extracted with CH_2Cl_2/H_2O. The organic layer was collected, dried over $MgSO_4$, and CH_2Cl_2 was removed by rotary evaporator. The residue was washed with diethyl ether and dried at 60 °C under vacuum for 4 h. The orange brown powder was obtained. Yield: 40 mg (87%).

: Anal. Calcd for $C_{34}H_{16}F_6N_2Pt$: C, 53.62.; H, 2.12; N, 3.68. Found: C, 53.44; H, 1.84; N, 3.49%. FT-IR (KBr, cm^{-1}) ν(-CF_3): 1163, 1120, ν(C≡C): 2117, ν(≡C-H): 3307. UV/VIS (CH_2Cl_2): λ_{abs} nm ($\varepsilon \times 10^{-5}$) 275 (0.66), 284 (0.70), 311 (0.46), 445 (0.07). ^{1}H NMR (CD_2Cl_2, 400 MHz, ppm): δ = 9.85 (d, J = 1.6 Hz, 2H, Phen-H2 and H9), 8.69 (d, J = 1.6 Hz, 2H, Phen-H4 and H7), 7.98 (s, 2H, Phen-H5 and H6), 7.61 (d, J = 8.6 Hz, 4H, Ph-H3 and H5), 7.58 (d, J = 8.6 Hz, 4H, Ph-H2 and H6), 3.64 (s, 2H, Phen≡H).

*2.2.7. Preparation of Pt(3,8-Phen≡H)(≡Ph-4-NO_2)$_2$ (**7H**)*

The Pt(3,8-Phen≡H)(≡Ph-4-NO_2)$_2$ was synthesized with 0.06 mmol scale by the same procedure to that for **1H** except for the use of **5TMS** (53 mg, 0.06 mmol). The orange powder is obtained. Yield: 42 mg (99%).

: Anal. Calcd for $C_{32}H_{18}N_4O_4Pt$: C, 53.71; H, 2.25; N, 7.83. Found: C, 53.44; H, 2.54; N, 7.62%. FT-IR (KBr, cm^{-1}) ν(-NO_2): 1337, ν(C≡C): 2112, ν(≡C-H): 3280. UV/VIS (CH_2Cl_2): λ_{abs} nm ($\varepsilon \times 10^{-5}$) 286 (0.34), 346 (0.51), 438 (0.09). ^{1}H NMR (CD_2Cl_2, 400 MHz, ppm): δ = 9.93 (d, J = 1.6 Hz, 2H, Phen-H2 and H9), 8.78 (d, J = 1.6 Hz, 2H, Phen-H4 and H7), 8.18 (d, J = 8.8 Hz, 4H, Ph-H3 and H5), 8.05 (s, 2H, Phen-H5 and H6), 7.66 (d, J = 8.8 Hz, 4H, Ph-H2 and H6), 3.66 (s, 2H, Phen≡H).

*2.2.8. Preparation of Pt(3,8-Phen≡H)(≡Ph-4-COOMe)$_2$ (**8H**)*

The Pt(3,8-Phen≡H)(≡Ph-4-COOMe)$_2$ was synthesized with half scale by the same procedure to that for **1H** except for the use of **8TMS** (89 mg, 0.10 mmol). The yellow powder is obtained. Yield: 68 mg (92%).

: Anal. Calcd for $C_{36}H_{22}N_2O_4Pt$ 1/2CH_2Cl_2: C, 55.91; H, 2.96; N, 3.57. Found: C, 55.87; H, 3.02; N, 3.63%. FT-IR (KBr, cm^{-1}) ν(C=O): 1713, ν(C≡C): 2113, ν(-CH_3): 2900, 2950, ν(≡C-H): 3241. UV/VIS (CH_2Cl_2): λ_{abs} nm ($\varepsilon \times 10^{-5}$) 288 (0.58), 322 (0.73), 453 (0.06). ^{1}H NMR (CD_2Cl_2, 400 MHz, ppm): δ = 10.01 (d, J = 1.6 Hz, 2H, Phen-H2 and H9), 8.77 (d, J = 1.6 Hz, 2H, Phen-H4 and H7), 8.04 (s, 2H, Phen-H5 and H6), 7.97 (d, J = 8.2 Hz, 4H, Ph-H3 and H5), 7.60 (d, J = 8.2 Hz, 4H, Ph-H2 and H6), 3.89 (s, 6H, $COOCH_3$), 3.65 (s, 2H, Phen≡H).

*2.2.9. Preparation of Pt(3,8-Phen≡H)(≡Ph-4-t-Bu)$_2$ (**9H**)*

The Pt(3,8-Phen≡H)(≡Ph-4-*t*-Bu)$_2$ was synthesized with 0.06 mmol scale by the same procedure to that for **6H** except for the use of **9TMS** (53 mg, 0.06 mmol). The dark brown powder is obtained. Yield: 43 mg (96%).

: Anal. Calcd for $C_{40}H_{34}N_2Pt$ 1/8CH_2Cl_2: C, 64.39; H, 4.61; N, 3.74. Found: C, 64.35; H, 4.67; N, 3.74%. FT-IR (KBr, cm^{-1}) ν(C≡C): 2116, ν(-CH_3): 2866, 2961, ν(≡C-H): 3308. UV/VIS (CH_2Cl_2): λ_{abs} nm ($\varepsilon \times 10^{-5}$) 258 (0.53), 284 (0.57), 318 (0.31), 466 (0.05). ^{1}H NMR (CD_2Cl_2, 400 MHz, ppm): δ = 9.99 (d, J = 1.6 Hz, 2H, Phen-H2 and H9), 8.64 (d, J = 1.6 Hz, 2H, Phen-H4 and H7), 7.97 (s, 2H, Phen-H5 and H6), 7.46 (td, J = 2.0, 8.8 Hz, 4H, Ph-H2 and H6), 7.38 (td, J = 2.0, 8.8 Hz, 4H, Ph-H3 and H5), 3.63 (s, 2H, Phen≡H)., 1.36 (s, 18H, *t*-Bu).

*2.2.10. Preparation of Pt(3,8-Phen≡H)(≡Ph-3,5-CF_3)$_2$ (**10H**)*

The Pt(3,8-Phen≡H)(≡Ph-3,5-CF_3)$_2$ was synthesized with 0.06 mmol scale by the same procedure to that for **6H** except for the use of **10TMS** (63 mg, 0.06 mmol). The black powder is obtained. Yield: 50 mg (92%).

: Anal. Calcd for $C_{36}H_{14}F_{12}N_2Pt_2$: C, 48.17; H, 1.57; N, 3.12. Found: C, 48.19; H, 1.77; N, 2.95%. FT-IR (KBr, cm^{-1}) ν(-CF_3): 1181, 1131, ν(C≡C): 2112, 2143, ν(≡C-H): 3310. UV/VIS (CH_2Cl_2): λ_{abs} nm ($\varepsilon \times 10^{-5}$) 274 (0.50), 284 (0.51), 308 (0.37), 328 (0.23), 342 (0.20), 435 (0.06). ^{1}H NMR (CD_2Cl_2, 400 MHz, ppm): $\delta = 9.93$ (d, $J = 1.6$ Hz, 2H, Phen-H2 and H9), 8.76 (d, $J = 1.6$ Hz, 2H, Phen-H4 and H7), 8.00 (s, 2H, Phen-H5 and H6), 7.94 (s, 4H, Ph-H2 and H6), 7.71 (s, 2H, Ph-H4), 3.64 (s, 2H, Phen≡H).

*2.2.11. Preparation of Pt(3,8-Phen≡H)(≡Ph-3,5-*t*-Bu)$_2$ (**11H**)*

The Pt(3,8-Phen≡H)(≡Ph-3,5-*t*-Bu)$_2$ was synthesized with 0.06 mmol scale by the same procedure to that for **6H** except for the use of **11TMS** (60 mg, 0.06 mmol). The orange-red powder is obtained. Yield: 43 mg (84%).

: Anal. Calcd for $C_{48}H_{50}N_2Pt$ 1/4CH_2Cl_2: C, 66.52; H, 5.84; N, 3.22. Found: C, 66.76; H, 5.87; N, 3.23%. FT-IR (KBr, cm^{-1}) ν(C≡C): 2111, ν(-CH_3): 2867, 2961, ν(≡C-H): 3312. UV/VIS (CH_2Cl_2): λ_{abs} nm ($\varepsilon \times 10^{-5}$) 258 (0.44), 284 (0.47), 318 (0.28), 466 (0.05). ^{1}H NMR (CD_2Cl_2, 400 MHz, ppm): $\delta = 10.13$ (d, $J = 1.7$ Hz, 2H, Phen-H2 and H9), 8.74 (d, $J = 1.7$ Hz, 2H, Phen-H4 and H7), 8.02 (s, 2H, Phen-H5 and H6), 7.46 (d, $J = 2.0$ Hz, 4H, Ph-H2 and H6), 7.32 (d, $J = 2.0$ Hz, 2H, Ph-H4), 3.60 (s, 2H, Phen≡H), 1.38 (s, 36H, *t*-Bu).

3. Results and discussion

3.1. Synthesis and characterization of platinum complexes

The 11 new platinum complexes, Pt(3,8-Phen≡H)(≡Ph-R)$_2$: R = H (**1H**), 4-F (**2H**), 3-F (**3H**), 2-F (**4H**), 4-Me (**5H**), 4-CF_3 (**6H**), 4-NO_2 (**7H**), 4-COOMe (**8H**), 4-*t*-Bu (**9H**), 3,5-di-CF_3 (**10H**), 3,5-di-*t*-Bu (**11H**), were difficult to obtain with a similar transmetalation method of Pt(3,8-Phen≡TMS)(≡Ph-R)$_2$ reported in our previous paper, because the starting complex Pt(3,8-Phen≡H)Cl_2 was not dissolved in major organic solvents [16]. So, we first tried to synthesize the present complexes by the ligand exchange reaction between Pt(COD)(≡Ph-R)$_2$ and 3,8-Phen≡H. This synthetic method produced some compounds (**3H** (67%), **4H** (53%), **5H** (39%), **10H** (29%)) in moderate yields, but other compounds were obtained at low yields under 15%. Then, the present complexes as shown in Scheme 1 were synthesized from the platinum complexes Pt(3,8-Phen≡TMS)(≡Ph-R)$_2$: R = H (**1TMS**), 4-F (**2TMS**), 3-F (**3TMS**), 2-F (**4TMS**), 4-Me (**5TMS**), 4-CF_3 (**6TMS**), 4-NO_2 (**7TMS**), 4-COOMe (**8TMS**), 4-*t*-Bu (**9TMS**), 3,5-di-CF_3 (**10TMS**), 3,5-di-*t*-Bu (**11TMS**) by a deprotection reaction of the trimethylsilyl group in high yields over 80%. All complexes were characterized by IR, ^{1}H NMR, UV–Vis, luminescence spectroscopy, and elemental analysis. The platinum organometallics exhibited ^{1}H NMR signals, and the elemental analysis results were in accordance with the assigned structures presented in Scheme 1.

The IR spectra of the present complexes indicated the η^1 coordination of metal–carbon bonds between the Pt atom and the ethynyl functional group of each of the 11 arylethynyl ligands. The characteristic strong ν(C≡C) bands assigned to the Pt-C≡C bonds of the complexes **1H**–**11H** were observed at around 2115 cm^{-1} (among 2111-2123 cm^{-1}) except for platinum complex **10H**, which had two peaks, at 2112 and 2143 cm^{-1}. These ν(C≡C) peaks of the Pt–C≡C bond in **1H**–**11H** were almost consistent with those of the precursor complexes **1TMS** – **11TMS** [16]. In addition, the peak for ν(CC-H) of 3,8-Phen≡H was observed at around 3300 cm^{-1} in the IR spectra of **1H**–**11H**. The ^{1}H NMR measurements support the formation of the H–C≡C bond in the phenanthroline ligand. A new assignable signal for the ethynyl proton of diethynylphenanthroline in the ^{1}H NMR spectra of **1H**–**11H** was detected at around 3.64 ppm, and the assignable signal for trimethylsilyl substituents was not observed. The proton signals assignable to the phenanthroline and arylethynyl ligands in **1H**–**11H** clearly showed similar chemical shift values in the respective precursors **1TMS** – **11TMS**, and therefore it was supported that the compounds had similar coordination structures to the precursor complexes under the deprotection reaction.

Fig. 1 shows the absorption spectra of **1H**–**11H** in CH_2Cl_2. These platinum organometallics with 11 arylethynyl ligands each have a broad absorption band over 360 nm, and this band was primarily assigned to the mixed transition of both the MLCT from platinum ion to the 3,8-Phen≡H and the LLCT from the respective arylethynyl ligands to the 3,8-Phen≡H ligand. The absorption bands of these complexes in the 300–350-nm region were primarily assigned to the lowest π-π^*(3,8-Phen≡H) and π-π^*(-≡-C_6H_4R) singlet transitions. The lowest-energy ^{1}[π-π^*(3,8-Phen≡H)] transition in each of these complexes was observed in the short wavelength area compared to the ^{1}[π-π^*(3,8-Phen≡TMS)] transition in each of precursor complexes. The lowest 1[π-π^*(-≡-C_6H_4R)] transition bands of the respective arylethynyl ligands with carboxy methyl ester and nitro substituents in **7H** and **8H** were observed in the 300–380 nm region. These assignments are consistent with those in **7TMS** and **8TMS**. The band of the mixed transition from ^{1}MLCT/^{1}LLCT over 400 nm in these platinum organometallics confirmed a hypsochromic effect of the present arylethynyl ligands in these organometallics. For example, **10H** with two trifluoromethyl substituents as an electron-withdrawing group exhibited an absorption band (435 nm) of the ^{1}MLCT/^{1}LLCT transition in the short wavelength area compared to the band (469 nm) of the same transition in **5H** with a methyl substituent as an electron-donating group.

3.2. Luminescence of *1H–11H* in solution state

Platinum complexes, **1H**–**11H**, each showed a visible broad emission band in deoxygenated CH_2Cl_2 at room temperature upon excitation at 425 nm, as shown in Fig. 2, while the emission spectra at 77 K in deoxygenated 2-Me-THF for these complexes each showed a high-intensity emission band with clear vibronic

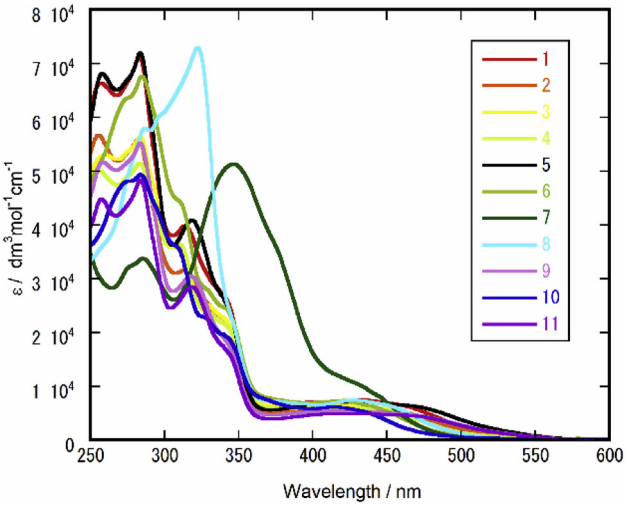

Fig. 1. UV–Vis absorption spectra of platinum organometallics **1H**–**11H** in CH_2Cl_2 at room temperature.

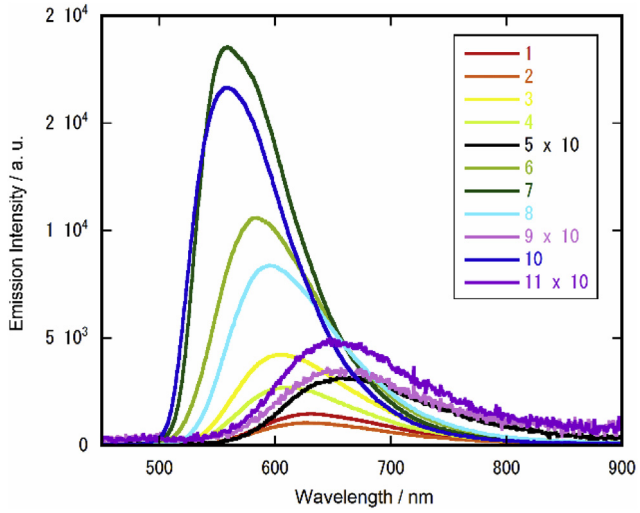

Fig. 2. Luminescence spectra of platinum organometallics **1H**–**11H** in CH_2Cl_2 at room temperature.

progressions in the high-energy region (Fig. 3). These emissions are assigned to phosphorescence from the triplet state of the mixed transition from MLCT and LLCT, namely ^{3}MLCT/^{3}LLCT, which is well known to be present in the luminescence for similar platinum(II) organometallic complexes with bipyridine derivatives and two various arylethynyl ligands, Pt(bipyridine derivatives)(≡-aryl)$_2$ [10–15]. The maximum intensity peaks of the emission band (λ_{em}) at room temperature in deoxygenated CH_2Cl_2 and those at 77 K in deoxygenated 2-MeTHF for these complexes are listed in Table 1. The peak wavelength values show that the complexes with an electron-withdrawing group are smaller, and have higher-energy values, than those with an electron-donating group. This trend is consistent with the tendency of the mixed transition of ^{1}MLCT/^{1}LLCT in UV–Vis spectra. The values at room temperature span a wide range, 559–664 nm, while those at 77 K are in a narrow region, 511–562 nm. These results in solution showed an emission color of yellow to red in the visible region. The emission quantum yields (ϕ_{em}) calculated by the standard relative method and luminescence life times (τ_{em}) at room temperature are also listed in Table 1. Interestingly, ϕ_{em} increased with decreasing λ_{em} from 664 nm to 559 nm for **1H**–**11H**. This result could be assumed to be caused by the so-called energy gap law because all of the platinum complexes present, as shown in Scheme 1, were very similar structures [15].

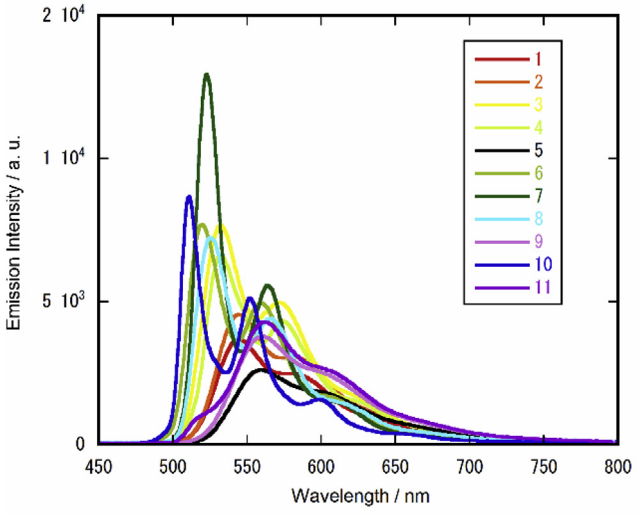

Fig. 3. Luminescence spectra of platinum organometallics **1H**–**11H** in 2-MeTHF at 77 K.

The trend of the maximum peak wavelength of the ^{3}MLCT/^{3}LLCT transition in the present organometallics was also strongly related to the energy separation between the excited triplet (T_1) state and the ground (S_0) state obtained by DFT and TD-DFT calculations. The DFT and TD-DFT calculations of the present organometallics aid the interpretation of the electronic effects of their aryl groups with different substituents on phosphorescence in CH_2Cl_2 at room temperature. An interesting finding is the good linear correlation between the emission energy values of the maximum intensity peak in the phosphorescent band, E_{em}, and the $E(T_1\text{-}S_0)_{DFT}$ or $E(T_1\text{-}S_0)_{TD\text{-}DFT}$ in terms of eV, as shown in Fig. 4. The energy separation between the T_1 state and the S_0 state, $E(T_1\text{-}S_0)_{DFT}$, was obtained as the difference between the HOMO energy level under the S_0 state and the highest SOMO energy level under the T_1 state, while the value of the direct T_1–S_0 transition energy, $E(T_1\text{-}S_0)_{TD\text{-}DFT}$, was obtained from the TD-DFT calculation in CH_2Cl_2. The calculated results of $E(T_1\text{-}S_0)_{DFT}$ and $E(T_1\text{-}S_0)_{TD\text{-}DFT}$ also are listed in Table 1. This linear correlation between the observed emission data and the calculated results by DFT and TD-DFT precisely underscores that the related MOs obtained by these calculations reflect the actual MOs in the present organometallics.

3.3. *Color and luminescence of platinum complexes, **1H**–**11H** and **1TMS** – **11TMS**, in solid state*

The color under white light (upper) and luminescent color under UV light (lower) of 22 platinum complexes, **1H**–**11H** and **1TMS** – **11TMS**, in solid state are shown in Fig. 5. For same sample condition, all solid samples were performed by the reprecipitation from CH_2Cl_2 solution and dried at 60 °C under vacuum for 4 h. These samples were measured by TG-DTA measurement and confirmed that the weight of these samples was not reduced until 150 °C as shown in supplementary data. The color of some complexes (**9H**, **10H**, **3TMS**, **8TMS**, **11TMS**) in solid was dark red, while the color of these complexes in solution ranged from yellow to orange. The definitive difference in color between solid state and in solution for these square planar platinum complexes is related to the influence of the Pt-Pt and π-π interactions in solid state, and the color change is a general phenomenon of the bathochromic effect resulting from these interactions, as reported [10–14]. On the other hand, the colors of the three compounds (**1H**, **8H**, **10TMS**) in solid state were almost the same as the yellow and yellow-orange of these complexes in solution, and the luminescent colors of **8H** and **10TMS** under UV light were orange and yellow. The bright emissions of two compounds, **8H** and **10TMS,** under UV light motivated us to measure the luminescent spectra of 22 platinum complexes in solid state.

The emission spectra of complexes **1H**–**11H** in solid state are shown in Fig. 6. The maximum intensity peaks in the short wavelength area less than 690 nm were observed only in the spectra of **1H** (609 nm, weak emission) and **8H** (684 nm; the spectrum showed a broad emission band from 500 nm to 850 nm). The maximum peaks of the other complexes were observed in long wavelengths over 690 nm; the longest wavelength value was 764 nm in **10H**, although the emissions of **2H** and **4H** were very weak and may have been in the short wavelength area. The emission maximum peaks of **1H**–**11H** in solution are between 560 nm and 660 nm, as listed in Table 1. The emissions of **1H**–**11H** in solution are assigned to the luminescence from the ^{3}MLCT/^{3}LLCT transition in the present organometallics mentioned above. So, it is

Table 1
Luminescence data and emission energy calculated by DFT and TD-DFT of platinum organometallics **1H**–**11H**.

Compound	Emission					DFT and TD-DFT data	
	λ_{em}/nm	λ_{em}/nm	ϕ_{em}[a]/%	τ_{em}/μs	E_{em}[b]/eV	$E(T_1\text{-}S_0)_{DFT}$	$E(T_1\text{-}S_0)_{TD\text{-}DFT}$
	at r.t.	at 77 K	at r.t.	at r.t.	at r.t.	(eV)	(eV)
1H	629	544	5.0	0.214	1.97	1.81	1.94
2H	631	544	4.7	0.172	1.97	1.82	1.93
3H	604	533	12.6	0.708	2.05	1.90	2.04
4H	610	532	8.5	0.488	2.03	1.90	2.02
5H	664	560	1.3	0.055	1.87	1.75	1.86
6H	585	520	28.0	1.332	2.12	1.98	2.11
7H	559	522	40.1	1.144	2.22	2.10	2.21
8H	595	525	23.0	1.033	2.08	1.97	2.09
9H	660	561	1.7	0.061	1.88	1.76	1.87
10H	559	511	36.8	1.655	2.22	2.05	2.20
11H	655	562	2.2	0.076	1.89	1.78	1.88

[a] Emission quantum yields (ϕ_{em}) were calculated relative to $[Ru(bpy)_3](PF_6)_2$ in a degassed acetonitrile ($\phi_{em} = 0.095$) as a standard.
[b] Wavelengths of emission maxima are converted to eV ($E_{em} = 1240/\lambda_{em}$).

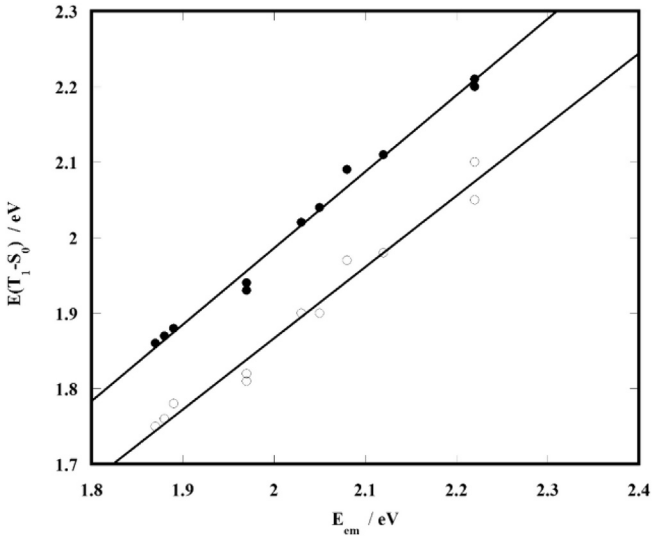

Fig. 4. Plots of the emission energy of the maximum intensity peak in the phosphorescent band, E_{em}, and the $E(T_1\text{-}S_0)_{DFT}$ from DFT (open circle) or $E(T_1\text{-}S_0)_{TD\text{-}DFT}$ from TD-DFT (black circle) in terms of eV.

presumable that strong emissions of several complexes (**3H**, **5H**, **6H**, **8H**, **10H**, **11H**), whose maximum peaks are over 690 nm, can be assigned to the luminescence from the ^{3}MMLCT transition in solid state because some kinds of similar platinum(II) organometallic complexes Pt(bipyridine derivatives)(≡-aryl)$_2$ in solid state have showed red emission from ^{3}MMLCT caused by the Pt-Pt interaction over 700 nm previously [10–15,17]. The molecular structures of the present platinum complexes are suitable for the Pt-Pt interaction in solid state, because the flat square planar structure is preferable to the stacking structure of the molecular plane in solid state. The weak emissions of the less-hindered complexes (**1H**, **2H**, **4H**) might be assigned to the luminescence from the ^{3}MLCT/^{3}LLCT transition because their emission spectra were similar to those of these complexes in solution (Fig. 2). Furthermore, the emission spectrum of **8H** might be included in the mixture luminescence from the ^{3}MLCT/^{3}LLCT and ^{3}MMLCT transitions in solid state.

The emission spectra of complexes **1TMS** – **11TMS** in solid state are shown in Fig. 7. The maximum peaks of many complexes were observed in the long wavelength area over 720 nm except for those of three complexes: **1TMS**, **10TMS**, and **11TMS**. The emissions of the maximum peaks over 720 nm can be assigned to the luminescence from the ^{3}MMLCT transition in solid state, as mentioned above. The emission maximum peak values of **1TMS** (597 nm), **10TMS** (573 nm), and **11TMS** (662 nm) in solid state are similar to those of **1TMS** (624 nm), **10TMS** (540 nm), and **11TMS** (650 nm), respectively, in solution, and the emission in solid state could be assigned to the phosphorescence from the ^{3}MLCT/^{3}LLCT transition or the mixture luminescence from the ^{3}MLCT/^{3}LLCT and ^{3}MMLCT transitions. This result presumes that the three complexes are situated no or weak Pt-Pt interaction in solid state. Because the strong π-π interaction between the molecules induces the molecules to overlap each other with a slight lateral shift in solid state and therefore the Pt-Pt interaction of the vertical direction against the molecular plane sometimes is weaken. The distinct vibronic emission spectrum of **10TMS**, whose luminescent colors under UV light were only bright yellow in the present 22 complexes, was observed. The shortest wavelength value of several peaks in the spectrum of **10TMS** was 528 nm, and this value was close to the emission maximum peak value of **10TMS** (518 nm) at 77 K in MeTHF. This similarity must indicate that **10TMS** in solid state was densely packed relative to the less-hindered complexes (**1H**, **2H**, **4H**, **1TMS**), which showed weak emissions from the ^{3}MLCT/^{3}LLCT transition, and the strong emission of **10TMS** compared to that of **1TMS** would be caused by the AIE effect in solid state. The complexes **1H** and **1TMS** were the least bulky in their respective complex series. We therefore assumed that the complexes could be formed by strong π-π interaction. However, the emission intensity from the ^{3}MLCT/^{3}LLCT transition of these complexes was very weak, and no distinct AIE effect was observed. This result reflects that the AIE effect for the present square-planar platinum complex system is not simple, as the complex that has a less-hindered ligand is introduced by the strong AIE effect. The arrangement of the arylethynyl ligand is most important for dense packing in the space of a crystal, because the AIE is caused by the suppression of the vibration and rotation of the compound under a photo-excited state from many previous AIE researches [19]. The **10TMS** must fill a void compared to the other, less-hindered complexes **1H** and **1TMS**.

4. Conclusion

A new series of platinum(II) diethynylphenanthroline complexes, Pt(3,8-Phen≡H)(≡Ph-R)$_2$, of 11 arylethynyl ligands with different substituents: R = H (**1H**), 4-F (**2H**), 3-F (**3H**), 2-F (**4H**), 4-Me (**5H**), 4-CF_3 (**6H**), NO_2 (**7H**), 4-COOMe (**8H**), 4-*t*-Bu (**9H**), 3,5-di-CF_3 (**10H**), 3,5-di-*t*-Bu (**11H**), was synthesized from a previous series of platinum(II) complexes, Pt(3,8-Phen≡TMS)(≡Ph-R)$_2$

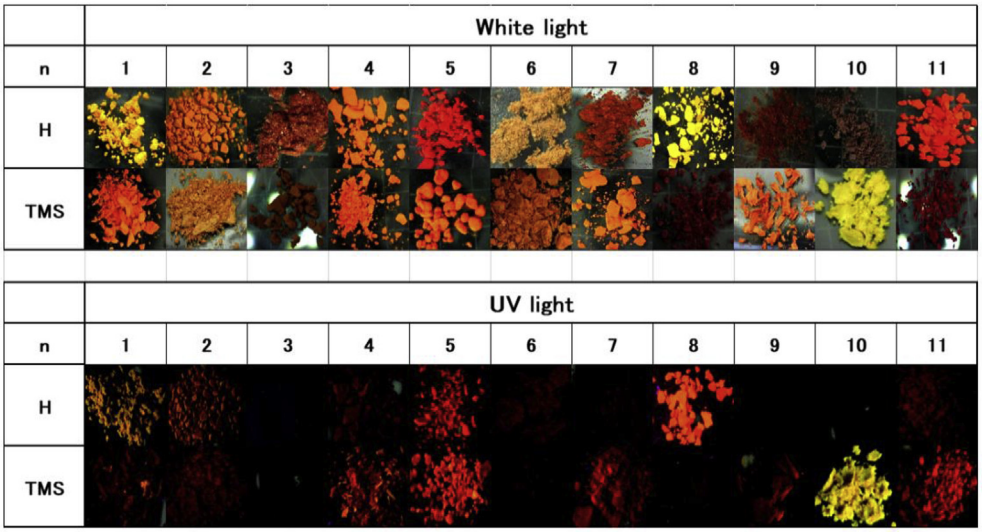

Fig. 5. Pictures of color (upper) under white light and luminescence (lower) under UV light of 22 platinum organometallics **1H**–**11H** and **1TMS** – **11TMS**. (For interpretation of the references to color in this figure legend, the reader is referred to the Web version of this article.)

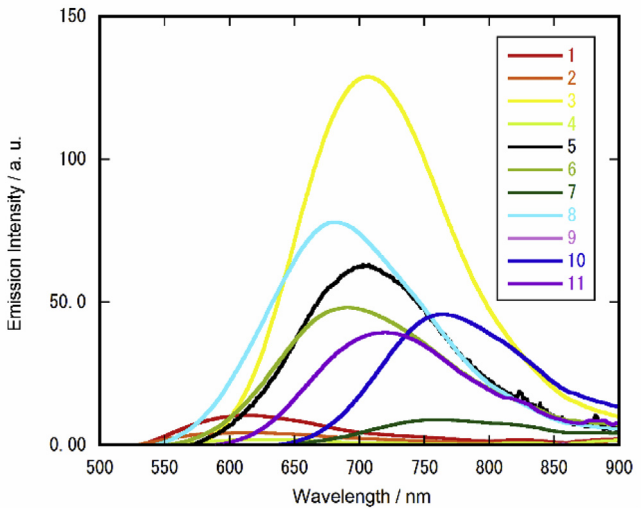

Fig. 6. Luminescence spectra of platinum organometallics **1H**–**11H** under solid state at room temperature.

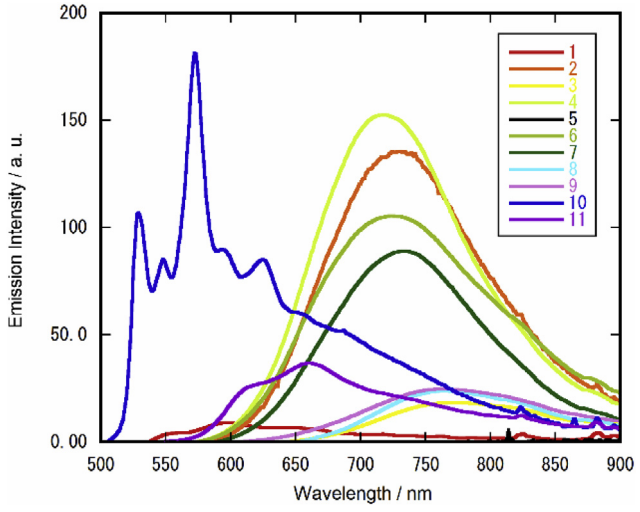

Fig. 7. Luminescence spectra of platinum organometallics **1TMS** – **11TMS** under solid state at room temperature.

(**1TMS** – **11TMS**), by a deprotection reaction of a trimethylsilyl group. The organometallics **1H**–**11H** showed absorption and emission spectra similar to those of respective precursor complexes **1TMS** – **11TMS** in solution. The emissions of all 22 platinum organometallics in solution were assigned to the phosphorescence from the mixed transition of the ^{3}MLCT/^{3}LLCT transition. A good linear correlation was obtained between the observed emission energy values of phosphorescence and the calculation values of the difference between the lowest excited triplet state and the ground singlet state by DFT or TD-DFT.

In solid state, the emission maximum peaks in the spectra of many complexes in the 22 platinum organometallics appeared in the long wavelength area over 700 nm. It is reasonable to support an assignment of the luminescence from the ^{3}MMLCT transition caused by the Pt-Pt interaction in the present platinum complex series. The intermolecular orientation of these complexes is related to the diversity of the intermolecular interactions as Pt-Pt and π–π interactions in solid state. The molecular structures of two platinum complex series are suitable for Pt-Pt interaction in solid state, because the flat square planar complex is preferable to the stacking structure in solid state. However, the less-hindered complex of **1TMS** and the complex with bulky ligands of **10TMS** respectively showed short wavelength emissions from the ^{3}MLCT/^{3}LLCT transition in solid state. So, the structural factor of each arylethynyl ligand sensitively affects the intermolecular packing and the luminescence of their complexes. Complex **10TMS** showed a particularly strong and vibronic emission. This phenomenon is presumed to be attributable to the AIE effect.

We are currently extending our photophysical research to study the solid state luminescence and vapochromism including a new series of platinum(II) phenanthroline complexes.

Acknowledgements

This work was supported by JSPS KAKENHI Grant Number JP17H06375 from Japan Society for the Promotion of Science, Japan.

Appendix A. Supplementary data

Supplementary data to this article can be found online at https://doi.org/10.1016/j.jorganchem.2018.10.032.

References

[1] (a) Y. Li, L. Chen, Y. Ai, E.Y.-H. Hong, A.K.-W. Chan, V.W.-W. Yam, J. Am. Chem. Soc. 139 (2017) 13858–13866;
(b) C. Shi, Q. Li, L. Zou, Z. Lv, A. Yuan, Q. Zhao, Eur. J. Inorg. Chem. 2018 (2018) 1131–1136;
(c) Y. Cheng, L. Li, F. Wei, K.M.-C. Wong, Inorg. Chem. 57 (2018) 6439–6446.

[2] (a) K. Li, G.S.M. Tong, Q. Wan, G. Cheng, W.-Y. Tong, W.-H. Ang, W.-L. Kwong, C.-M. Che, Chem. Sci. 7 (2016) 1653–1673;
(b) D. Nolan, B. Gil, L. Wang, J. Zhao, S.M. Draper, Chem. Eur J. 19 (2013) 15615–15626.

[3] (a) A. Kobayashi, M. Kato, Eur. J. Inorg. Chem. 2014 (2014) 4469–4483;
(b) F.K.-W. Hau, H.-S. Lo, V.W.-W. Yam, Chem. Eur J. 22 (2016) 1–13;
(c) I. Stengel, C.A. Strassert, E.A. Plummer, C.-H. Chien, L. De Cola, P. Bäuerle, Eur. J. Inorg. Chem. 2012 (2012) 1795–1809.

[4] (a) K.T. Ly, R.-W. Chen-Cheng, H.-W. Lin, Y.-J. Shiau, S.-H. Liu, P.-T. Chou, C.-S. Tsao, Y.-C. Huang, Y. Chi, Nat. Photon. 11 (2016) 63–68;
(b) H.-X. Shu, J.-Y. Wang, Q.-C. Zhang, Z.-N. Chen, F, Inorg. Chem. 56 (2017) 9461–9473;
(c) X. Cui, J. Zhao, Z. Mohmood, C. Zhang, Chem. Rec. 16 (2016) 173–188;
d) W.-Y. Wong, C.-L. Ho, J. Mater. Chem. 19 (2009) 4457–4482;
e) W.-Y. Wong, C.-L. Ho, Coord. Chem. Rev. 253 (2009) 1709–1758;
f) G. Zhou, W.-Y. Wong, S. Suo, J. Photochem, C. Photobio, Photochem. Rev. 11 (2010) 133–156;
g) G. Zhou, W.-Y. Wong, X. Yang, Chem. Asian J. 6 (2011) 1706–1727.

[5] (a) Y. Ma, P. She, K.Y. Zhang, H. Yang, Y. Qin, Z. Xu, S. Liu, Q. Zhao, W. Huang, Nat. Commun. 9 (2018) 1–7;
(b) M. Lahav, M.E. van der Boom, Adv. Mater. (Weinheim, Ger.) 1706641 (2018) 1–7;
c) L. Ying, C.-L. Ho, H. Wu, Y. Cao, W.-Y. Wong, Adv. Mater. (Weinheim, Ger.) 26 (2014) 2459–2473;
d) X. Yang, G. Zhou, W.-Y. Wong, J. Mater. Chem. C 2 (2014) 1760–1778;
e) X. Xu, X. Yang, J. Zhao, G. Zhou W.-Y. Wong, Asian J. Org. Chem. 4 (2015) 394–429;
f) C.-L. Ho, W.-Y. Wong, New J. Chem. 37 (2013) 1665–1683;
g) C.-L. Ho, W.-Y. Wong, Coord. Chem. Rev. 257 (2013) 1614–1649.

[6] (a) M. Yoshida, M. Kato, Coord. Chem. Rev. 355 (2018) 101–115;
(b) J.A.G. Williams, Top. Curr. Chem. 257 (2005) 1–32;
(c) V.W.-W. Yam, K.M.-C. Wong, Top. Curr. Chem. 281 (2007) 205–268.

[7] (a) S. Carrara, A. Aliprandi, C.F. Hogan, L. De Cola, J. Am. Chem. Soc. 139 (2017) 14605–14610;
(b) M.E. Robinson, A. Nazemi, D.J. Lunn, D.W. Hayward, C.E. Boott, M.-S. Hsiao, R.L. Harniman, S.A. Davis, G.R. Whittell, R.M. Richardson, L. De Cola, I. Manners, ACS Nano 11 (2017) 9162–9175.

[8] (a) H.-K. Cheng, M.C.-L. Yeung, V.W.-W. Yam, ACS Appl. Mater. Interfaces 9 (2017) 36220–36228;
(b) F.K.-W. Hau, H.-S. Lo, V.W.-W. Yam, Chem. Eur J. 22 (2017) 1–13.

[9] (a) W. Yang, J. Zhao, Eur. J. Inorg. Chem. 2016 (2016) 5283–5299;
(b) Z. Li, Y. Han, Z. Gao, F. Wang, ACS Catal. 7 (2017) 4676–4681;
(c) Z.-L. Gong, Y.-W. Zhong, J. Yao, J. Mater. Chem. C 5 (2017) 7222–7229;
(d) C.-J. Lin, Y.-H. Liu, S.-M. Peng, T. Shinmyozu, J.-S. Yang, Inorg. Chem. 56 (2017) 4978–4989.

[10] (a) J. Ni, Y.-G. Wang, H.-H. Wang, Y.-Z. Pan, L. Xu, Y.-Q. Zhao, X.-Y. Liu, J.-J. Zhang, Eur. J. Inorg. Chem. 2014 (2014) 986–993;
(b) J. Ni, Y.-G. Wang, J.-Y. Wang, Y.-Q. Zhao, Y.-Z. Pan, H.-H. Wang, X. Zhang, J.-J. Zhanga, Z.-N. Chen, Dalton Trans. 42 (2013) 13092–13100;
(c) X. Zhang, J.-Y. Wang, J. Ni, L.-Y. Zhang, Z.-N. Chen, Inorg. Chem. 51 (2012) 5569–5579;
(d) J. Ni, X. Zhang, Y.-H. Wu, L.-Y. Zhang, Z.-N. Chen, Chem. Eur J. 17 (2011) 1171–1183;
(e) J. Ni, X. Zhang, N. Qiu, Y.-H. Wu, L.-Y. Zhang, J. Zhang, Z.-N. Chen, Inorg. Chem. 50 (2012) 9090–9096;
(f) J. Ni, Y.-H. Wu, X. Zhang, B. Li, L.-Y. Zhang, Z.-N. Chen, Inorg. Chem. 48 (2008) 10202–10210.

[11] J. Ni, L.-Y. Zhang, H.-M. Wena, Z.-N. Chen, Chem. Commun. (J. Chem. Soc. Sect. D) 25 (2009) 3801–3803.

[12] Z.M. Hudson, C. Sun, K.J. Harris, B.E.G. Lucier, R.W. Schurko, S. Wang, Inorg. Chem. 50 (2011) 3447–3457.

[13] K.-C. Chang, J.-L. Lin, Y.-T. Shen, C.-Y. Hung, C.-Y. Chen, S.-S. Sun, Chem. Eur J. 18 (2012) 1312–1321.

[14] Y. Li, A.Y.-Y. Tam, K.M.-C. Wong, W. Li, L. Wu, V.W.-W. Yam, Chem. Eur J. 17 (2011) 8048–8059.

[15] (a) M. Hissler, W.B. Connick, D.K. Geiger, J.E. McGarrah, D. Lipa, R.J. Lachicotte, R. Eisenberg, Inorg. Chem. 39 (2000) 447–457;
(b) S.-C. Chan, M.C.W. Chan, Y. Wang, C.-M. Che, K.-K. Cheung, N. Zhu, Chem. Eur J. 7 (2001) 4180–4190;
(c) C.E. Whittle, J.A. Weinstein, M.W. George, K.S. Schanze, Inorg. Chem. 40 (2001) 4053–4062;
(d) W. Lu, M.C.W. Chan, N. Zhu, C.-M. Che, Z. He, K.-Y. Wong, Chem. Eur J. 9 (2003) 6155–6166.

[16] M. Shiotsuka, T. Asano, Y. Kurono, R. Ono, R. Kawabe, J. Organomet. Chem. 851 (2017) 1–8.

[17] J. Ni, J.-J. Kang, H.-H. Wang, X.-Q. Gai, X.-X. Zhang, T. Jia, L. Xu, Y.-Z. Pan, J.-J. Zhang, RSC Adv. 5 (2015) 65613–65617.

[18] M.J. Frisch, G.W. Trucks, H.B. Schlegel, G.E. Scuseria, M.A. Robb, J.R. Cheeseman, G. Scalmani, V. Barone, B. Mennucci, G.A. Petersson, H. Nakatsuji, M. Caricato, X. Li, H.P. Hratchian, A.F. Izmaylov, J. Bloino, G. Zheng, J.L. Sonnenberg, M. Hada, M. Ehara, K. Toyota, R. Fukuda, J. Hase-gawa, M. Ishida, T. Nakajima, Y. Honda, O. Kitao, H. Nakai, T. Vreven, J.A. Montgomery Jr., J.E. Peralta, F. Ogliaro, M. Bearpark, J.J. Heyd, E. Broth-ers, K.N. Kudin, V.N. Staroverov, R. Kobayashi, J. Normand, K. Raghava-chari, A. Rendell, J.C. Burant, S.S. Iyengar, J. Tomasi, M. Cossi, N. Rega, J.M. Millam, M. Klene, J.E. Knox, J.B. Cross, V. Bakken, C. Adamo, J. Jaramillo, R. Gomperts, R.E. Stratmann, O. Yazyev, A.J. Austin, R. Cammi, C. Pomelli, J.W. Ochterski, R.L. Martin, K. Morokuma, V.G. Zakrzewski, G.A. Voth, P. Salvador, J.J. Dannenberg, S. Dapprich, A.D. Daniels, Ö. Farkas, J.B. Foresman, J.V. Ortiz, J. Cioslowski, D.J. Fox, Gaussian 09,Revision C.01, Gaussian, Inc., Wallingford, CT, 2011.

[19] (a) M. Gao, B.Z. Tang, ACS Sens. 2 (2017) 1382–1399;
(b) J. Mei, N.L.C. Leung, R.T.K. Kwok, J.W.Y. Lam, B.Z. Tang, Chem. Rev. 115 (2015) 11718–11940;
(c) J. Mei, Y. Hong, J.W.Y. Lam, A. Qin, Y. Tang, B.Z. Tang, Adv. Mater. (Weinheim, Ger.) 26 (2014) 5429–5479.